# The Impact of Camber Variation on NACA 2412 Airfoil Efficiency and Its Implications for Adaptive Engineering Solutions


## ABSTRACT

This paper investigates the effects of varying the camber on the aerodynamic efficiency of the NACA 2412 airfoil by analyzing the Lift-to-Drag (L/D) ratio. Using wind tunnel tests at a constant speed of 95 MPH, data was collected for different camber configurations, and L/D ratios were computed for each trial. The NACA 2412 airfoil camber was modified to increase the camber by 20%, decrease it by 20%, and decrease surface area by 20%. These were all tested at Angle of Attack values from 0 to 30 in 5-degree increments. The results revealed a strong correlation between camber variation and aerodynamic efficiency, with certain camber settings significantly enhancing performance at specific Angles of Attack.While the original NACA 2412 served as a control, modifications such as reduced camber and surface area demonstrated significant efficiency changes, underscoring the role of camber in optimizing performance. The study provides valuable insights for optimizing airfoil design, offering practical applications in aircraft engineering, particularly in the development of systems that can adapt wing geometry dynamically to optimize performance. However, limitations such as fixed airspeed and limited camber variations were noted, highlighting the need for further investigation into more diverse conditions. These findings contribute to a broader understanding of how engineering solutions can enhance aircraft performance by incorporating adaptable design elements.



*Keywords: Airfoil efficiency, Applied engineering, Aviation, Firmware, Engineering, Aerospace,*


## 1. INTRODUCTION

Research question: To what extent does the changing of camber impact the efficiency of NACA 2412 airfoils, as measured by the Lift to Drag Ratio?

**Background Information:**

This investigation focuses on the NACA 2412 airfoil, specifically, an existing airfoil shape designed by the National Advisory Committee for Aeronautics (NACA), the precursor to NASA. The '2412' designation focuses on specific geometric characteristics (Othman and Al-Obaidi 2).

The efficiency of an airfoil, measured by its Lift-to-Drag (L/D) ratio, is highly influenced by both its geometric configuration and its interaction with airflow. In this study, the focus ison the impact of changing camber on the efficiency of the NACA 2412 airfoil. The camber, which is the curvature of the airfoil, plays a significant role in generating lift and controlling drag. By exploring how varying the camber affects the L/D ratio, valuable insights can be gained into optimizing aerodynamic performance.

In modern aircraft, this optimization is increasingly driven by intelligent firmware systems that adjust wing geometry in real time. Firmware-controlled mechanisms allow for dynamic camber adjustment based on flight conditions, enabling a more responsive and efficient airfoil. This study's findings on camber-induced efficiency shifts can guide the development of such firmware systems, ensuring that airfoil performance remains optimal across a wide range of angles of attack and flight speeds. Integrating aerodynamic


UNDER PEER REVIEW

principles with firmware design contribute to the advancement of adaptive wing technologies, improving both aircraft performance and fuel efficiency."

The Angle of Attack, also called the Angle of Incidence, refers to the angle formed by the chord and direction of the relative wind. The Critical Angle of Attack occurs when the airflow from the upper airfoil surface separates or detaches from the wing. As the AoA increases by increasing the airfoil's angle, the airflow encounters a point where it can no longer follow the contour of the wing. This leads to Stalls (a dramatic loss of Lift) and increases the induced component of Drag.

According to Bernoulli's principle, as the air velocity increases along an airfoil's surface, the pressure along the surface decreases (Matsson et al. 8). Additionally, as the Angle of Attack of an airfoil increases, the separation between the airfoil's upper and lower sections pressures' increases and leads to a strong lifting force (Liu 10).

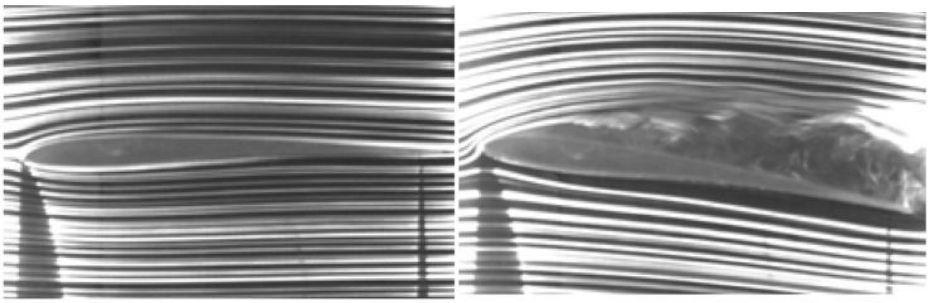


Figure 1. Airflow separation as AoA increases (Anyoji and Hamada 78)

The lift force (L) acting on an airfoil is described in the following formula:

$L = \frac{1}{2} \cdot Cl \cdot \rho \cdot A \cdot V^2$

L is the lift force, Cl is the Coefficient of Lift (a dimensionless constant), ρ is the air density, A is the wing area, and V is the air velocity. Lift is a force that acts perpendicular to the motion between the airfoil and the surrounding air (Gibbs 27).

Analyzing the coefficient of lift distribution helps understand the performance of an airfoil with different modifications, such as changes in AoA or surface modifications. The higher the Cl of an airfoil (airspeed, and air density constant), the higher the amount of Lift (per unit) is produced (Othman and Al-Obaidi 8).

Drag, the resistive force opposing thrust, is influenced by factors such as airfoil shape and surface roughness (Gibbs 4). Parasitic Drag is Drag caused by non-lift components, such as the fuselage and protruding portions of aircraft. Interference Drag is the type of Drag created by various aircraft components, like the wings, elevators, and stabilizers (Gibbs 6). Drag opposes Lift and decreases the Lift to Drag ratio, impacting overall efficiency.Interference Drag is the type of Drag created by various aircraft components, like the wings, elevators, and stabilizers (Gibbs 6). Drag opposes Lift and decreases the Lift to Drag ratio, impacting overall efficiency.

The Lift to Drag Ratio (L/D) acting on an airfoil is described in the following formula:

$L/D = Lift/Drag$

$Lift/Drag = Cl(\frac{1}{2} \cdot \rho \cdot A \cdot V2) / Cd(\frac{1}{2} \cdot \rho \cdot A \cdot V^2)$

UNDER PEER REVIEW

Where Cl is the Coefficient of Lift and Cd is the Coefficient of Drag. The L/D ratio measures how effectively an airfoil produces lift while minimizing drag, a resistive force ("Lift to Drag"). A high L/D ratio implies that the airfoil produces a substantial lift force while minimizing drag, enhancing overall efficiency (Anyoji and Hamada 77).

**Hypothesis**:

Building upon the research above, it can be hypothesized that decreasing the camber of NACA 2412 airfoils will increase its Lift to Drag Ratio and overall airfoil efficiency. This will be seen as an increase in the Lift to Drag ratio and a larger Critical Angle of Attack (Angle of Incidence). Additionally, a concave down parabolic relationship can be expected between the L/D Ratio and AoA with the vertex representing the Critical Angle of Attack being met.

## 2. METHODOLOGY

Independent Variables:Camber of the airfoil tested in the wind tunnel:
x: 0.0933 m, y: 0.0096 m, z: 0.075 m (Airfoil A: NACA 2412 with 20% reduction thickness camber)
x:0.0933 m, y: 0.0096 m, z: 0.012 m (Airfoil B: NACA 2412 original dimensions)
x: 0.0933 m, y: 0.0144 m, z: 0.075 m (Airfoil C: NACA 2412 with 20% thicker camber)
x:0.0746 m, y: 0.0096 m, z: 0.06 m (Airfoil D: NACA 2412 with 20% surface area reduction).
All measurements were made with a micrometer with an error margin of  25 micrometers.

Dependent Variables:  The Lift and Drag Coefficients that the airfoil produces when measured in by the Jet Stream 500 wind tunnel, with an error margin of  0.0001.

Controlled Variables:

- Windspeed (Controlled value: 95  0.01 MPH)
  - Wind speed impacts Lift and Drag, so by keeping the wind speed constant, the effects of camber on the lift and drag coefficients canbe isolated.
- The Angle of Attack (Range from 0-30 Degrees +/- 0.1 Deg during testing)
  - Repeating constant Angle of Attack checkpoints (0-30 Degrees) for each Airfoil reduces variability and allows concrete comparison points to graph objectively.
- Air Temperature Inside the Wind Tunnel
  - Temperature changes can affect air density, a key player in the Lift formula detailed above. Keeping it constant allows the reduction of extraneous variables.
- 3D Printing Software and Material
  - Differences in surface roughness can increase Skin Friction Drag, so standardizing the 3D printing method and material ensures consistency.

### 2.1 Apparatus:

- 3D Printed Airfoil A (NACA 2412 with 20% reduction thickness camber)
  - Dimensions*: x: 0.0933 m, y: 0.0096 m, z: 0.075 m*
- 3D Printed Airfoil C (NACA 2412 with 20% thicker camber)
  - Dimensions: x: 0.0933 m, y: 0.0144 m, z: 0.075 m
- 3D Printed Airfoil B (NACA 2412 original dimensions)
  - Dimensions: x: 0.0933 m, y: 0.0096 m, z: 0.012 m
- 3D Printed Airfoil D (NACA 2412 with 20% surface area reduction)
  - Dimensions: x: 0.0746 m, y: 0.0096 m, z: 0.06 m
- Jet Stream 500 wind tunnel (length: 6' 2", depth: 18", height: 23")
- Console Display Station
- Laptop

UNDER PEER REVIEW

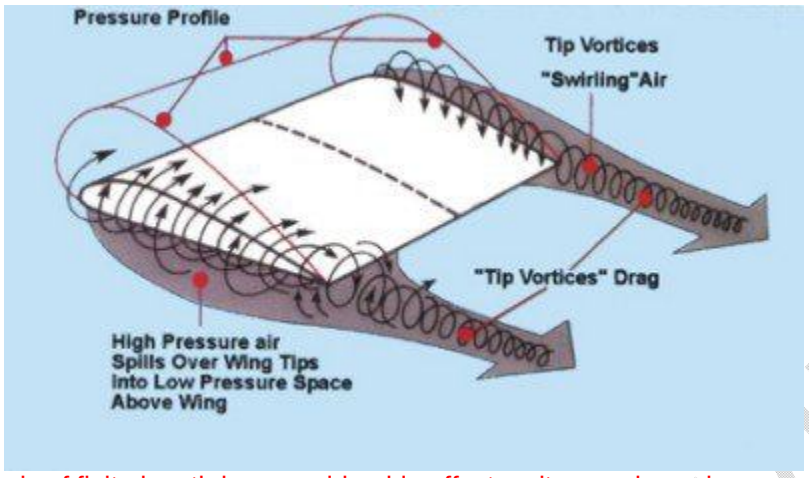


The fact that a wing is of finite length has considerable effect on its aerodynamic properties. The primary effect is due to the span-wise lift distribution (it is no longer constant), caused by the flow about the wing tips. In normal operating conditions, the wing will have high pressure on its lower surface and a low pressure on its upper surface. This pressure difference is what generates the lift. However, this same pressure difference causes flow from the under side of the wing to the upper side of the wing around the wing tips. This type of flow swirls off the tips of the wing in the form of vortices. In fact, there is a vortexdistribution across the entire span of the wing with the strongest vortices at the wing tips. Thesevortices trail downstream behind the wing and rotate in the direction shown in the figure.Vortices on the right-hand side of the wing (looking from the rear) rotate counter clockwise, andthose on the left-hand side of the wing rotate clockwise. The general result is that the vorticesinduce a downward flow at the wing interior. This downward flow is called downwash, and it influences the flow in front of, at, and behind the wing. This downward flow causes a change in the local wing angle-of-attack such that the wing sees a different angle-of-attack then the one that it sees with respect to the free stream.

Figure 3. Apparatus Setup (Generated by Candidate)

UNDER PEER REVIEW

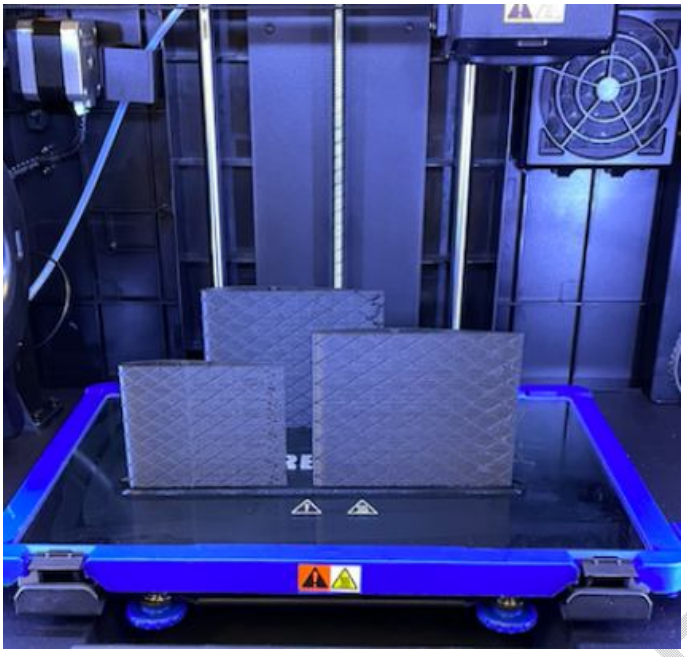

Figure 3. 3D printed Airfoils (Generated by Candidate)


Figure 4. Set up of Experiment

(Generated by Candidate)

### 2.2 Procedure:

1. Set up the apparatus as shown in the diagram (Figure2) using Airfoil A, making sure that screws secure the airfoil, and the console display & Jet Seam Program are connected.

UNDER PEER REVIEW

2. Adjust the Angle of Attack (between 0 and 30 Deg) manually in the testing chamber to 0 degrees.
3. Set the wind speed setting on the console to 95 MPH and start the program.
4. Monitor the console, record the Lift and Drag Coefficient measurements on the laptop.
5. Once data from the target airspeed (95 MPH) is reached, the program on the laptop can be stopped and results collected.
6. Repeat two more times with the same Angle of Attack and Airfoil.
7. Adjust the Angle of attack +5 degrees manually in the testing chamber and repeat steps 3-7 with the same Airfoil until the Angle of Attack reaches 30 Degrees.
8. Repeat steps 1-7 with Airfoils B, C, and D.

### 2.3 Safety Precautions:

The safety concerns in this experiment are low, aside from the potential risk of hearing damage due to the elevated noise levels within the wind tunnel. The experiment occurred in a sealed testing chamber, ensuring a sterile environment and the location was deliberately isolated from standard workstations. Ethical and environmental considerations are insignificant, as the wind tunnel and 3D printing processes operate on a conservative amount of electricity.
Experimental Uncertainty: Data was collected through a digital measurement system with an uncertainty of 0.0001 (according to the official Jet Steam 5000 manual). The Angle of Attack to the nearest Degree was altered manually between trials, allowing an uncertainty of 0.1 Degree. This uncertainty can affect the accuracy of results as they are used in future calculations and have an extensive range.

### 2.4 DataCollection and Processing

Sample Raw Data:
The table below displays sample data for Airfoil D. Appendix A shows the remaining Data Tables for Airfoil A, B, and C.

| Airfoil D | Lift± 0.000001 | | | Drag± 0.000001 | | |
|---|---|---|---|---|---|---|
| AoA0.1 Deg | Trial 1 | Trial 2 | Trial 3 | Trial 1 | Trial 2 | Trial 3 |
| 0 Deg | 0.005728 | 0.005951 | 0.005978 | 0.019417 | 0.019812 | 0.019824 |
| 5 Deg | 0.050806 | 0.051848 | 0.051808 | 0.02242 | 0.022249 | 0.023013 |
| 10 Deg | 0.080867 | 0.081474 | 0.083407 | 0.025912 | 0.025923 | 0.026898 |
| 15 Deg | 0.184874 | 0.187962 | 0.191532 | 0.051268 | 0.051869 | 0.053146 |
| 20 Deg | 0.275297 | 0.238905 | 0.261839 | 0.072135 | 0.072204 | 0.074355 |
| 25 Deg | 0.197828 | 0.201013 | 0.208039 | 0.051464 | 0.052649 | 0.053394 |
| 30 Deg | 0.225812 | 0.229089 | 0.231953 | 0.073331 | 0.074576 | 0.075648 |

Table 1. Raw Data Table (6 decimal places) for AIRFOIL D, measured with Jet Stream 500 application

| **Sample Averages Calculation for Airfoil D** | **Sample Abs. Unc. Calculation for Airfoil D** |
|---|---|
| To average values, sum all the values across 3 trials for a given Angle of Attack divided by the number of trials conducted.<br><br>*A=Sum of all observations/Total number of* | Absolute Uncertainty is found by dividing the range of the data set by 2. |

UNDER PEER REVIEW

| | |
|---|---|
| *observations* $=a1+a2+...+an/n$<br>Ex: 15° AoA: Lift Coefficient<br>$(0.184874+0.187962+0.191532)/3$<br>$=0.18878$<br>Ex: 15° AoA: Drag Coefficient<br>$(0.051268+0.051869+0.053146)/3$<br>$=0.05242$ | Ex: 15° AoA: Lift Coefficient<br>$(0.191532-0.184874)/2$<br>$=0.003329$<br><br>Ex: 15° AoA: Drag Coefficient<br>$(0.053146-0.051268)/2$<br>$=0.000939$ |

Since experimental uncertainty is limited to one significant figure, the value is 0.003 for Lift and 0.001 for Drag. The significant figures of the uncertainty value determine the number of digits to be represented in the value it relates to. As a result, the final values are as follows.

**Lift Coefficient: 0.189 ±0.003** **Drag Coefficient: 0.052 ± 0.001**

**Sample L/D Ratio Calculations for Airfoil D:**

The Lift to Drag Ratio is the measurement of the efficiency of an airfoil, found by dividing the Lift Coefficient by the Drag Coefficient. A high ratio indicates a highly efficient Airfoil (produces more Lift than Drag), and a low (or negative) ratio suggests a lack of efficiency as there is more Drag than is preferred.

$$L/D=Lift/Drag$$

$$Lift/Drag=Cl(\tfrac{1}{2}\cdot \rho\cdot A\cdot V^2)/Cd(\tfrac{1}{2}\cdot \rho\cdot A\cdot V^2) = Cl/Cd$$

A few common factors in the numerator and denominator can be canceled out since the air density ($\rho$), wing area ($A$), and velocity of the air ($V$) are constant during testing. The simplified equation is as follows.

$$Lift/Drag=Cl(\cancel{\tfrac{1}{2}\cdot \rho\cdot A\cdot V^2})/Cd(\cancel{\tfrac{1}{2}\cdot \rho\cdot A\cdot V2}) = Cl/Cd$$

**Ex: 15° AoA:** The coefficients of Lift and Drag are 0.18878 and 0.05242, respectively.

$$L/D=0.18878/0.05242$$
$$=3.601$$

The L/D Ratio is a unitless measure, so it provides a dimensionless quantity representing an airfoil's efficiency.

L/D Processed Data Tables for Airfoil A, B, and C are located in Appendix A.

**2.5 Processed Data:**

| AoA | Avg. Lift | Abs. Unc. | Avg. Drag | Abs. Unc. | L/D Ratio |
|---|---|---|---|---|---|
| 0 | 0.006 | 0.0001 | 0.01968 | 0.0002 | 0.29834 |
| 5 | 0.05150 | 0.0005 | 0.02256 | 0.0003 | 2.28072 |

UNDER PEER REVIEW

| | | | | | |
|---|---|---|---|---|---|
| 10 | 0.08191 | 0.001 | 0.02624 | 0.0005 | 3.11684 |
| 15 | 0.18878 | 0.003 | 0.05243 | 0.001 | 3.60576 |
| 20 | 0.23834 | 0.02 | 0.07256 | 0.001 | 3.74112 |
| 25 | 0.20296 | 0.005 | 0.05283 | 0.001 | 3.84251 |
| 30 | 0.22861 | 0.003 | 0.07451 | 0.001 | 3.06557 |

Table 2. Processed Data Table with Averages and Abs. Unc. for AIRFOIL D

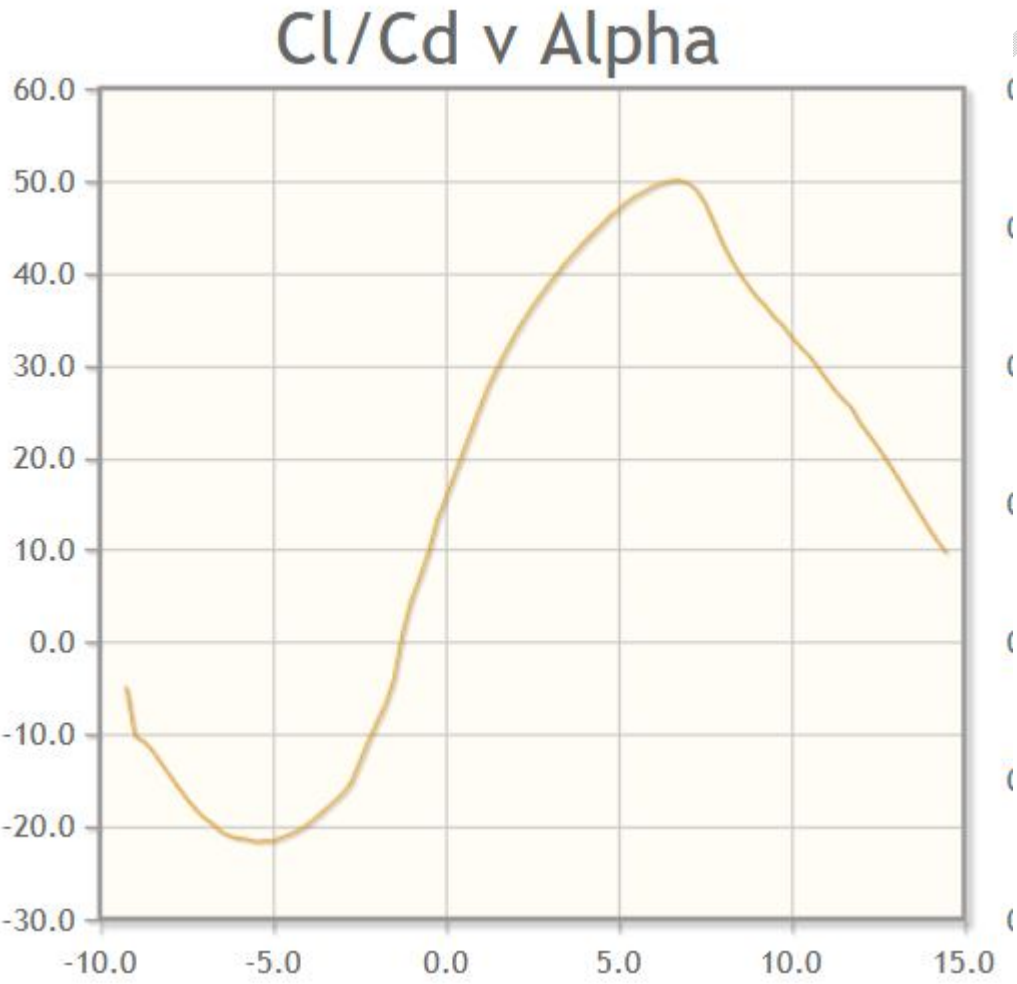


**Lift to Drag ratio for NACA 2412 - NACA 2412 airfoil at Re=100 000**

The Lift to Drag Ratio was then graphed against the Angle of Attack for the 4 airfoil samples and the trends are displayed below.

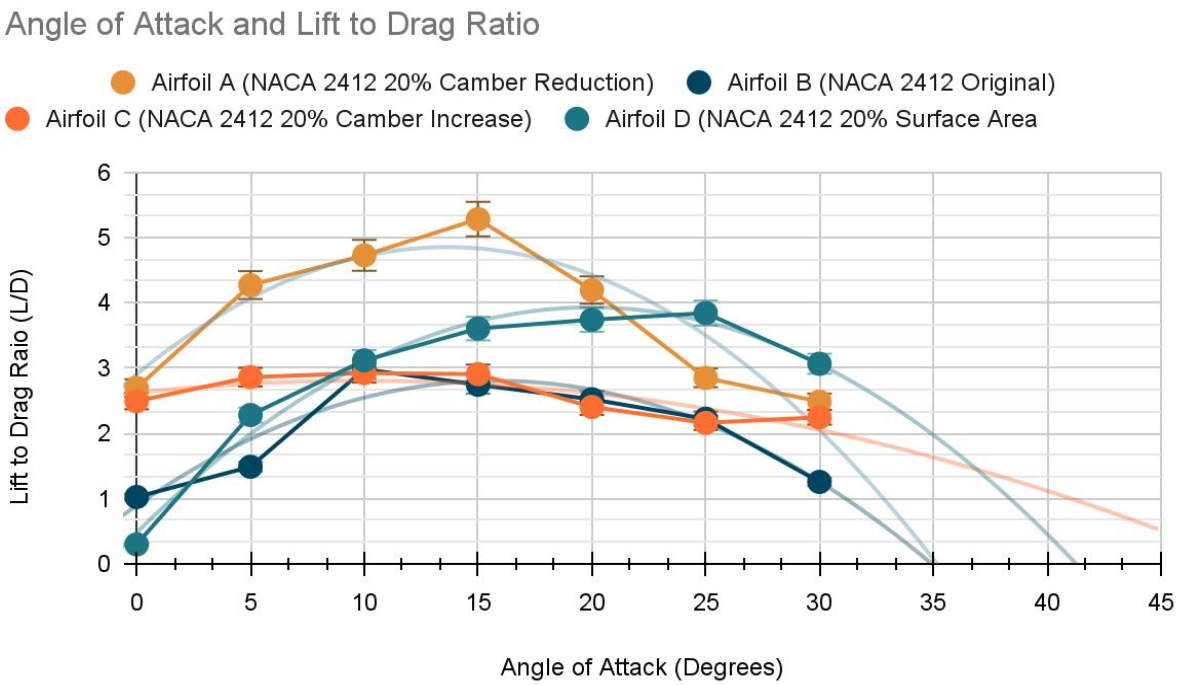


Figure 5. L/D Ratio vs Angle of Attack with Best-Fit Curve and Error Bars for all 4 Airfoils

The graph displays a parabolic trend between the L/D Ratio and AoA, increasing until the Critical Angle of Attack is met and then declining. Additionally, the graph shows Airfoil A as having the best L/D Ratio and efficiency. Airfoil A (*Dimensions: x: 0.0933 m, y: 0.0096 m, z: 0.075 m)* represents the NACA 2412 airfoil with a 20% reduction in camber (the data table for Airfoil A are present in Appendix A).

## 3 DISCUSSION AND ANALYSIS

This aligns with the hypothesis as decreasing the camber of NACA 2412 airfoils (Airfoil A) will increase its Lift to Drag Ratio and overall airfoil efficiency. Unlike in the hypothesis, decreasing the camber causes the Critical Angle of Attack to reduce. Airfoil A has a Critical AoA at 15 Degrees, the lowest of all tested airfoils.

Some contributors to the Lift-to-Drag (L/D) ratio include air density, surface area, and wind velocity. In the current experiment, using air with a constant velocity of 95 MPH and consistent air density allows for the substantial control of potential confounding variables. However, the intentional alteration of the surface area of Airfoil D, with a deliberate reduction of 20% compared to the original NACA 2412 design, aims to explore how changes in surface area influence aerodynamic performance.

As Airfoil A's Angle of Attack increases during testing, the Lift consistently increases to approximately 15 degrees, where it hits the Critical AoA, where efficiency is the highest. Anything beyond that point leads to a loss in Lift. This is shown by the decrease in the L/D Ratio and loss of efficiency as the Drag increases at a greater rate than the Lift. By 30 degrees of AoA, the L/D Ratio is roughly the same as 0 degrees, showing how the efficiency has diminished dramatically after the Angle of Incidence was passed.

Airfoil A is the NACA 2412 model with a 20% camber reduction, causing the breadth to change from 0.012 m to 0.075 m. It shows the most dramatic L/D Ratio and most pronounced parabolic trend. Airfoil B, the original NACA 2412 airfoil, acts as the control (see Appendix A for the data table). It has no altercations and serves as a baseline for the other airfoils.

UNDER PEER

Airfoil C, designed with a 20% increase in camber, exhibited a trend where the parabola experiences vertical compression compared to the patterns seen in other airfoils. Its performance curve was skewed, with less pronounced symmetry on the domain that was tested. Although its L/D ratio converged to a similar value as Airfoil A at an Angle of Attack of 30 degrees, it failed to achieve competitive efficiency overall. This suggests that the increased camber negatively impacted the airfoil's ability to balance lift and drag optimally, leading to diminished aerodynamic efficiency compared to the other configurations.

Airfoil D, characterized by a 20% dimension reduction, shows interesting results. Despite the smaller size and surface area, the L/D ratio remains competitive, and L/D values are comparable to and even exceed those of Airfoil B. This observation suggests that the L/D ratio remains consistent across varying surface areas. However, since Airfoil D is thinner than Airfoil B, with dimensions of *x: 0.0746 m, y: 0.0096 m, z: 0.06 m* compared to Airfoil B *( x: 0.0933 m, y: 0.0096 m, z: 0.012 m),* it achieves a slightly higher L/D ratio than the original. Notably, efficiency experiences a decline after 25 degrees of Angle of Attack, indicating an increase in the Critical Angle of Attack compared to the original. Overall, the results of Airfoil D's testing challenge initial expectations and highlight the significance of considering multiple factors, such as surface area, in aerodynamic analyses.

Our findings align with Khanna et al. (2024), who observed similar AoA efficiency trends in their study, further supporting the presence of a critical AoA where efficiency peaks.

The observed trends across all airfoils reinforce the complexity of aerodynamic interactions. For Airfoil A, the pronounced parabolic trend highlights the direct relationship between reduced camber and enhanced aerodynamic efficiency. Airfoil C's skewed trend and vertical compression further emphasize the delicate interplay between camber and aerodynamic forces. The inability of Airfoil C to maintain a competitive L/D ratio across the tested AoA range suggests diminishing returns from increased camber. Interestingly, Airfoil D's performance demonstrates that reductions in surface area do not proportionally reduce efficiency. Despite its smaller dimensions, Airfoil D maintained competitive L/D ratios, even surpassing Airfoil B in some cases.

The data also reveal critical inflection points across all airfoil configurations. These findings also prompt considerations for future investigations. The relatively narrow AoA range tested in this experiment limits broader conclusions about behavior at extreme negative or positive AoA. This study contributes to the growing understanding of how specific airfoil modifications impact aerodynamic performance, particularly in contexts requiring adaptable designs. In applications such as UAVs and aircraft with dynamically adjustable wings, leveraging these findings could inform the development of systems that optimize performance across varying flight conditions.

**Literature Review:**

The findings that camber adjustments significantly alter aerodynamic performance aligns with the findings from Raj & Rose (2022) and Karasu et al. (2020). Both papers emphasize the pivotal role of camber in improving lift-to-drag efficiency and minimizing flow separation. By increasing the camber ratio, the long laminar separation bubble observed in the airfoil transitions into a shorter bubble. These findings suggest that camber ratio adjustments can notably affect the aerodynamic performance of airfoils by altering critical flow phenomena.

The studies by Wang et al. (2022) and Ouro et al. (2018) extend this understanding by providing numerical simulations and experimental data on cambered airfoils, employing similar methodology involving controlled variables and wind tunnel testing. Ouro et al. discuss how cambered airfoils generally outperform symmetric airfoils in terms of L/D ratios due to higher lift generation. However, they caution that increased camber can lead to adverse effects like premature flow separation during dynamic operations. Jawahar et al. (2018) and Ouro et al. (2018) further illustrate the application of camber

variations in real-world scenarios, such as UAVs and wind turbines, drawing similar emphasis on engineering implications.

**Evaluation:**

In this study, the measured absolute uncertainty for Lift & Drag coefficients and the L/D Ratio was minimal, averaging at 0.003 and 0.0001, respectively. Despite this, challenges were encountered, particularly in dealing with uncertainties associated with the Angle of Attack measurement (±0.1 Degree) and air velocity (±0.1 MPH). The precision of these measurements is crucial, as even slight deviations can significantly impact the overall accuracy of the results. Potential fixes are upgrading to a higher-powered wind tunnel, conducting more trials (due to time, I conducted 3), and measuring the Angle of Attack with a precision protractor.

The airfoil construction process plays a crucial role in the potential introduction of errors. While the digital nature of the 3D printing process minimizes human error and provides precise control over dimensions using Blender software, imperfections may still arise. While the results demonstrate clear trends consistent with established aerodynamic principles, the observed trial discrepancies highlight the need for more precise experimental controls. Future investigations should incorporate automated AoA adjustments and higher-resolution instrumentation to minimize variability and enhance reproducibility

The data collected closely followed the parabolic best-fit curve, aligning with the expected trends, but there were some slight outliers. Furthermore, the parabolic trend cannot be guaranteed if the data is extrapolated to Angle of Attack values above 30 Degrees. In the conducted experiment, there is no evidence of a consistent intercept on the y or x-axis. The meticulous approach, involving multiple trials, careful adjustment of the Angle of Attack, and recalibration of the wind tunnel after each use, collectively minimized the likelihood of systematic inaccuracies in the experimental setup.

A few additional issues were noted while conducting the experiment, summarized in the bulleted list below. These might have contributed to the slight deviations in the experiment's results.

- Variability in Wind Tunnel Conditions: The variability in wind tunnel conditions introduces the possibility of errors, especially if the seal is imperfect. Imperfect sealing leading to air escaping could result in random errors, impacting air velocity.
- Pitot System Blockage: Blockages in the Pitot system, which is responsible for collecting air data after it passes over the airfoils, could impact all measurements. Depending on the cause of blockages, it could be either systematic (if consistently present) or random (if occasional and unpredictable).
- Equilibrium Position Alignment: The need to redo the setup for each trial may result in imperfect alignment of the equilibrium position (random error).

Differences between trials were observed, likely stemming from subtle alignment shifts during setup and minor variations in airfoil surface properties due to manufacturing tolerances. For instance, the 3D printing process introduces an average surface roughness variability of ±0.01 mm, potentially altering Drag coefficients at higher angles of attack. Additionally, wind tunnel flow stability, measured to ±0.1 MPH, may have introduced minor inconsistencies in force measurements.

The skewed trend observed in Airfoil C suggests an earlier transition to turbulent flow due to increased camber. This may exacerbate Drag forces and suppress Lift, explaining its poor performance relative to Airfoil A. These results are consistent with established aerodynamic models predicting adverse pressure gradients in over-cambered designs.

UNDER PEER REVIEW

## 4. CONCLUSION

To conclude, the experiment supports the hypothesis that variations in camber significantly impact the Lift-to-Drag (L/D) ratio, as exemplified by distinct trends in Airfoils A, B, and C. Airfoil D's performance also suggests that reduced surface area can influence aerodynamic efficiency in complex ways. Additionally, the critical angle of attack remains a crucial factor affecting the overall performance of the airfoils. These findings underscore the complexity of aerodynamic interactions.

### Further Research:

First, it is suggested that this experiment be carried out more than once or conducting simulations could provide a more comprehensive understanding and eliminate some of the extraneous variables present. It may also be worth investigating the specific effects on Drag and lift independently. It would be recommended to 3D print airfoils and sand them to reduce texture differences and roughness. Additionally, measuring the exact center points in the airfoils for the screws and rods ensures proper alignment.

The best-fit curve does not go through the origin, which was unexpected. The assumption had been made that an Angle of Attack of 0 would have also caused the L/D Ratio to have been zero. In further investigations, the Angle of Attack range will be extended to negative AoA (-15 to 30 Degrees total) to investigate the impact of negative Angle of Attack on the parabolic trend of the L/D Ratio.

From a technological perspective, further research could explore how these aerodynamic insights can be applied to the development of firmware-controlled adaptive wing systems. By leveraging real-time data such as airspeed, angle of attack, and pressure distribution, embedded systems can be designed to dynamically adjust the camber of the airfoil during flight. Such firmware-driven solutions would allow aircraft to continuously optimize their aerodynamic efficiency, leading to improved performance, reduced drag, and fuel savings. Testing these adaptive systems in simulated and real-world environments would be a logical next step to validate the potential of integrating firmware technology with aerodynamic design principles.

From an engineering perspective, further research could explore how these aerodynamic findings can be translated into innovative aircraft design practices. Technologies that enable real-time adjustments to wing geometry, based on changing flight conditions, could significantly improve aerodynamic performance and fuel efficiency. Future studies might focus on the development and testing of such adaptive systems, ensuring they are robust, efficient, and able to perform under a variety of conditions. This multidisciplinary approach, combining aerodynamics with innovative engineering solutions, could lead to significant advancements in aircraft performance and design.

Disclaimer (Artificial intelligence)

Option 1:

Author(s) hereby declare that NO generative AI technologies such as Large Language Models (ChatGPT, COPILOT, etc.) and text-to-image generators have been used during the writing or editing of this manuscript.

### References


1. "Aerodynamic pitching moment." *Flight Mechanics for Pilots*, 24 may 2020, agodemar.github.io/flightmechanics4pilots/mypages/pitching-moment/. Accessed 29 Dec. 2023.

2. "Angle of attack (aoa)." *SkyBrary*, skybrary.aero/articles/angle-attack-aoa. Accessed 7 Dec. 2023.

3. Anyoji, Masayuki, and Daiki Hamada. "High-performance airfoil with low reynolds-number dependence on aerodynamic characteristics. "*Fluid Mechanics Research International Journal*,


UNDER PEER REVIEW

vol. 3, no. 2, 19 aug. 2019, pp. 75-80. *research gate*, www.researchgate.net/profile/masayuki-anyoji/publication/346851605.pdf. Accessed 28 Sept. 2023.

4. Gibbs, Jason. *Experimental Determination of Lift and Lift Distributions for Wings in Formation Flight*. 2005. Virginia polytechnic institute and state university, Ms thesis. *v-tech works*, vtechworks.lib.vt.edu/server/api/core/bitstreams/484d9ae7-0533-411f-8988-6837c6d75319/content. Accessed 30 oct. 2023.

5. *Hasan Kamliya Jawahar et al. "Experimental and numerical investigation of aerodynamic performance for airfoils with morphed trailing edges." Renewable Energy (2018). https://doi.org/10.1016/J.RENENE.2018.04.066.*

6. *Ilyas Karasu et al. "EFFECTS OF THICKNESS AND CAMBER RATIO ON FLOW CHARACTERISTICS OVER AIRFOILS." Journal of Thermal Engineering (2020). https://doi.org/10.18186/thermal.710967.*

7. "Lift to drag ratio." *Glenn research center*, NASA, www1.grc.nasa.gov/beginners-guide-to-aeronautics/lift-to-drag-ratio/. Accessed 6 Sept. 2023.

8. Khanna, Amit, et al. “Temporary Empowerment: The Rise and Fall of the Women Airforce Service Pilots (WASPs) in Post-World War II America and Their Influence on Firmware Engineering Principles.” International Journal of Research Publication and Reviews, vol. 5, no. 11, 12 Nov. 2024, pp. 2391–2396, www.ijrpr.com/view.php?id=21735. Accessed 22 Nov. 2024.

9. Liu, Hansong. *Aerodynamic characteristics of the flat plate airfoil at low reynolds numbers*. 2021. The Johns Hopkins University, Ms Thesis. *J scholarship library*, jscholarship.library.jhu.edu/server/api/core/bitstreams/content. Accessed 3 Nov. 2023.

10. Matsson, John E., et al. "Aerodynamic Performance of the NACA 2412 airfoil at low Reynolds num- ber." *Semantics Scholar*, 26 june 2016, www.semanticscholar.org/paper/aerodynamic-performance-of-the-naca-2412-airfoil-at-matsson-voth. Accessed 26 Oct. 2023.

11. Othman, K. A., and A SMahdi Al-Obaidi. "Effect of the wing airfoil shape on the aerodynamics and performance of a jet-trainer aircraft – an optimization approach."*IOP Science*, vol. 2120, 30 June 2021, iopscience.iop.org/article. Accessed 30 Dec. 2023.

12. *P. Ouro et al. "Effect of Blade Cambering on Dynamic Stall in View of Designing Vertical Axis Turbines." Journal of Fluids Engineering-transactions of The Asme, 140 (2018): 061104. https://doi.org/10.1115/1.4039235.*

13. *R. J. Raj et al. "Flow physics and boundary layer optimization over a NACA airfoil by camber morphing at subsonic speeds." International Journal of Modern Physics C (2022). https://doi.org/10.1142/s0129183123500808.*

14. *Shuaishuai Wang et al. "Influence of camber on aerodynamic performance of airfoil based on CFD technology." Journal of Physics: Conference Series, 2276 (2022). https://doi.org/10.1088/1742-6596/2276/1/012027.*

UNDER PEER REVIEW

## APPENDIX

### Airfoil A

| 0.1 Deg | Lift | ± 0.0001 | | | Drag | ± 0.0001 | | | |
|---|---|---|---|---|---|---|---|---|---|
| AoA | Trial 1 | Trial 2 | Trial 3 | Avg. | Trial 1 | Trial 2 | Trial 3 | Avg. | L/D Ratio |
| 0 | 0.228825 | 0.228117 | 0.229344 | 0.228762 | 0.085057 | 0.084671 | 0.084814 | 0.084847 | 2.694157 |
| 5 | 0.113051 | 0.116344 | 0.117267 | 0.115554 | 0.026574 | 0.026574 | 0.027999 | 0.027049 | 4.270541 |
| 10 | 0.353564 | 0.358573 | 0.364028 | 0.358055 | 0.074598 | 0.075314 | 0.076427 | 0.075780 | 4.727545 |
| 15 | 0.4218 | 0.426289 | 0.431807 | 0.426632 | 0.079752 | 0.080792 | 0.081697 | 0.080747 | 5.281986 |
| 20 | 0.547543 | 0.558682 | 0.571914 | 0.559713 | 0.130689 | 0.133302 | 0.136238 | 0.133410 | 4.195598 |
| 25 | 0.663241 | 0.67638 | 0.682902 | 0.674174 | 0.232592 | 0.237222 | 0.240052 | 0.236622 | 2.849272 |
| 30 | 0.835119 | 0.847242 | 0.856986 | 0.846449 | 0.335203 | 0.340586 | 0.346519 | 0.340436 | 2.485964 |

### Airfoil B

| 0.1 Deg | Lift | ± 0.0001 | | | Drag | ± 0.0001 | | | |
|---|---|---|---|---|---|---|---|---|---|
| AoA | Trial 1 | Trial 2 | Trial 3 | Avg. | Trial 1 | Trial 2 | Trial 3 | Avg. | L/D Ratio |
| 0 | 0.05725 | 0.05690 | 0.05735 | 0.05712 | 0.05612 | 0.05634 | 0.05599 | 0.05626 | 1.02400 |
| 5 | 0.055433 | 0.058092 | 0.056293 | 0.056939 | 0.058092 | 0.028841 | 0.028841 | 0.038258 | 1.487538 |
| 10 | 0.165465 | 0.170372 | 0.168264 | 0.168700 | 0.05611 | 0.057047 | 0.056654 | 0.056604 | 2.981292 |
| 15 | 0.245501 | 0.250925 | 0.2492 | 0.248542 | 0.08984 | 0.091146 | 0.091729 | 0.090572 | 2.744198 |
| 20 | 0.314835 | 0.324861 | 0.31978 | 0.319825 | 0.124369 | 0.128485 | 0.126457 | 0.126770 | 2.520778 |
| 25 | 0.398578 | 0.40751 | 0.403021 | 0.403370 | 0.179131 | 0.18401 | 0.182258 | 0.181466 | 2.223114 |
| 30 | 0.469162 | 0.477814 | 0.472257 | 0.473744 | 0.373189 | 0.381857 | 0.377991 | 0.377679 | 1.255490 |

### Airfoil C

| 0.1 Deg | Lift | ± 0.0001 | | | Drag | ± 0.0001 | | | |
|---|---|---|---|---|---|---|---|---|---|
| AoA | Trial 1 | Trial 2 | Trial 3 | Avg. | Trial 1 | Trial 2 | Trial 3 | Avg. | L/D Ratio |
| 0 | 0.11561 | 0.11761 | 0.120258 | 0.117826 | 0.041199 | 0.042496 | 0.041437 | 0.042711 | 2.493209 |
| 5 | 0.10296 | 0.104776 | 0.106622 | 0.104786 | 0.035751 | 0.036141 | 0.036961 | 0.036618 | 2.861360 |
| 10 | 0.170422 | 0.173806 | 0.176214 | 0.173814 | 0.05828 | 0.059507 | 0.059629 | 0.059472 | 2.921873 |
| 15 | 0.213729 | 0.21683 | 0.219638 | 0.216732 | 0.07358 | 0.074772 | 0.075476 | 0.074609 | 2.906899 |
| 20 | 0.311731 | 0.318129 | 0.316033 | 0.315631 | 0.133849 | 0.131828 | 0.129885 | 0.131521 | 2.403776 |
| 25 | 0.349451 | 0.35707 | 0.363616 | 0.356046 | 0.162652 | 0.168688 | 0.165874 | 0.165071 | 2.160232 |
| 30 | 0.364883 | 0.364883 | 0.369203 | 0.366989 | 0.162796 | 0.165532 | 0.16096 | 0.163096 | 2.246313 |

UNDER PEER REVIEW